Comparison of JET-C DD neutron rates independently predicted by the ASCOT and TRANSP Monte Carlo heating codes

H. Weisen[1], P. Sirén[2,3], J. Varje[4,5]and JET Contributors[*]

[1]*Ecole Polytechnique Fédérale de Lausanne (EPFL), Swiss Plasma Center (SPC), CH-1015 Lausanne, Switzerland*

[2]*VTT Technical Research Centre of Finland, P.O Box 1000, 02044 VTT, Espoo, Finland*[2]

[3] *Helsinki University, Department of Applied Physics, P.O. Box 11000, FI-00076 Helsinki, Finland*

[4]*Aalto University, Espoo, Finland*
[5]*Tokamak Energy Ltd, Milton Park, OX14 4SD, United Kingdom*

[*] See the author list of "Overview of JET results for optimising ITER operation" by J. Mailloux et al. to be published in Nuclear Fusion Special issue: Overview and Summary Papers from the 28th Fusion Energy Conference (Nice, France, 10-15 May 2021)

Abstract. Simulations of the DD neutron rates predicted by the ASCOT and TRANSP Monte Carlo heating codes for a diverse set of JET-C (JET with carbon plasma facing components) plasmas are compared. A previous study [1] of this data set using TRANSP found that the predicted neutron rates systematically exceeded the measured ones by factors ranging between 1 and 2. No single explanation for the discrepancies was found at the time despite a large number of candidates, including anomalous fast ion loss mechanisms, having been examined. The results shed doubt on our ability to correctly predict neutron rates also in the Deuterium-Tritium plasmas expected in the JET D-T campaign (DTE2). For the study presented here the calculations are independently repeated using ASCOT with different equilibria and independent mapping of the profiles of temperature and density to the computational grid. Significant differences are observed between the results from the investigations with smaller systematic differences between neutron rates measurements and predictions for the ones using ASCOT. These are traced back not to intrinsic differences between the ASCOT and TRANSP codes, but to the differences in profiles and equilibria used. These results suggest that the discrepancies reported in ref. [1] do not require invoking any unidentified plasma processes responsible for the discrepancies and highlight the sensitivity of such calculations to the plasma equilibrium and the necessity of a careful mapping of the profiles of the ion and electron densities and temperatures.

1. Introduction

This paper is a sequel to a publication on the so-called 'neutron deficit' [1] in JET, defined as a systematic shortfall of the measured DD neutron rates with respect to those calculated by the TRANSP-NUBEAM [2-4] Monte Carlo orbit code. The fusion power produced in the plasma by neutronic fusion reactions such as the DD, DT and TT reactions, is directly proportional to the corresponding neutron rates. Hence our ability to measure, model and predict neutron rates is essential for predicting and understanding the results from the second high power JET Deuterium-Tritium campaign (DTE2) scheduled for the 2nd half of 2021 [5], as well as for the development of a future fusion reactor. The successful modelling of the neutron rate in an experimental fusion device

is also a very valuable indicator of the accuracy of the required experimental measurements, such as temperature and density profiles. While the knowledge of the existence of a shortfall of the measured neutron rates was available by word of mouth within the JET community since the nineties, it had not been systematically investigated before the study of ref [1]. In that study, data from a set of some 300 samples defined by averages over time intervals with stationary conditions of duration of order 1s were used. These plasmas, produced between 2001 and 2009, when JET was equipped with a carbon divertor and carbon limiters (JET-C), were neutral beam heated (NBH), with no or negligible ion cyclotron heating. The samples span a wide range of plasma conditions, including so-called "baseline" and "hybrid scenario" plasmas [6]. These scenarios are also planned for ITER operation and were developed in preparation for the DTE2 campaign [5]:

$0.8\text{MA} \delta I_p \delta 4\text{MA}$, $1\text{T} \delta B_T \delta 3.4\text{T}$, $2\ \text{MW} < P_{NBI} < 23\text{MW}$, $1.5\cdot10^{19} \delta \langle n_e \rangle \delta\ 9.4\cdot10^{19} \text{m}^{-3}$, $0.002 \delta \langle n_C \rangle / \langle n_e \rangle \delta 0.06$, $1.4 \delta Z_{eff}(\text{VB}) \delta 4$, $0.75 \delta q_0 \delta 2$, $2.4 \delta q_{95} \delta 5.4$, $0.06 \delta \tau_E \delta 0.5\text{s}$, $0.47 \delta \text{H98} \delta 1.4$

I_p is the plasma current, B_T the toroidal magnetic field, P_{NBI} the NBH power, $\langle n_e \rangle$ the volume average density, $\langle n_C \rangle$ the volume average carbon density from charge exchange spectroscopy (CXS) [7], Z_{eff}(VB) is the line average effective charge as measured by visible bremstrahlung, q_0 is the safety factor on the magnetic axis determined by the equilibrium code TEQ, which is used in TRANSP, q_{95} is the safety factor at 95% of the enclosed poloidal flux, τ_E is the energy confinement time based on the kinetic stored energy calculated from the plasma profiles and H98 is τ_E normalised to the IPB98(y,2) scaling [8]. The neutron rates from beam-thermal reactions were always dominant, ranging from 50% to 96% of the total neutron rate, the lower end of the range corresponding to plasmas with high power, high temperatures and moderate to low densities, such as hybrid scenario plasmas. The fraction of neutrons from thermal-thermal reactions ranged from near 1% at low temperatures to near 50% at high temperature and density. The beam-beam neutron rates represented a fraction in the range 1%-27% of the total, scaling with electron temperature and inversely with density.

The choice of JET-C data for that study [1] was motivated by the routine availability of ion temperature profiles obtained from visible charge exchange spectroscopy (CXS) using a C^{5+} line. The data from these plasmas are part of the JETPEAK database, which is described in refs [9 & 10]. The current study repeats these calculations using the ASCOT Monte Carlo orbit code [11,12] with inputs to ASCOT taken directly from JETPEAK.

This comparison between the TRANSP results from ref. [1] with the new ASCOT results must not be considered as a comparison between the two codes, but rather as a comparison between two entire analysis procedures using different codes and more importantly, different equilibria and different ways of fitting and mapping the same

input data. They show, in a perhaps sobering way, how different the results from different approaches can be. They also put into question the notion of a 'neutron deficit' and the hypothesis of the existence of unidentified plasma processes which might be at the origin of these discrepancies. In a previous detailed study [13] of two different discharges, a baseline and a low density hybrid scenario plasma from JET with an ITER-Like-Wall (JET-ILW, post 2010), predictions for DD neutron rates from ASCOT exceeded those from TRANSP by some 5% for the baseline case and 10% for the hybrid plasmas when the same equilibria and profiles were used. This is significantly less than the differences seen in the study at hand, especially for baseline plasmas. An explanation for the differences has so far not been found, although the observation that these differences are reduced when plasma bulk rotation is assumed to be zero, suggests that differences in the way the effects of plasma rotation are treated in the two codes may play a role [13].

2. Description of the TRANSP and ASCOT calculations

The data in JETPEAK, are, like those that were used in ref. [1], obtained from the JET processed pulse file (PPF) system and mapped and fitted to the computational grid using equilibria from the the EFIT code [14] generally used at JET. A major difference is that the TEQ code [4], which is integrated in TRANSP, was used for ref. [1]. (Importing the equilibria and profiles from the TRANSP output to be used as input for ASCOT calculations would allow a very broad-based benchmarking of the two codes for identical inputs, but is beyond the scope of this work. Software for importing TEQ equilibria into the JETPEAK-ASCOT environment is still to be created). Both codes used the guiding center approximation for representing the orbits of the slowing-down NBH-injected ions. Charge exchange losses were not calculated by ASCOT. They were for the TRANSP runs, however affecting only the outermost ~10% of the plasma cross section, which barely contributes to the total neutron rate. Both codes also use the same nuclear data in the form of parametric fits [15]. For the calculation of beam penetration and ionisation TRANSP made use of atomic coefficients obtained from ref [16], while ASCOT uses those from ADAS [17]. The difference between the two was found to be insignificant [1].

There are further significant differences between the way the current ASCOT and the original TRANSP calculations were performed. The TRANSP calculations were produced by a team of 7 TRANSP users over the course of several weeks, using exactly the same TRANSP run settings (i.e without individual adjustments to improve agreement with the experimental data) and using the same experimental JET input data, such as the carbon ion temperatures, rotation velocities and densities from CXS and electron temperatures from LIDAR Thomson scattering (see ref. [1] for details). These produced time resolved TRANSP results which were subsequently averaged over the stationary JETPEAK time windows and integrated into JETPEAK. By contrast, the time-averaged diagnostics data from the time windows are provided as inputs for automated ASCOT calculations, i.e for each sample, defined by a pulse number and a time window, only an ASCOT run for one slowing down time to thermalisation is

performed [13], rather than a dozen or more time steps for TRANSP. The number of tracer particles for ASCOT was set to 1000, which was found to be sufficient for calculating the beam-thermal neutron rates to a few percent. As a calculation for a single sample takes less than 10 minutes CPU time on the computers of the JET analysis cluster, all 300 ASCOT calculations were completed in under 3 days.

We wish to point out that in both TRANSP and JETPEAK the deuterium temperature is inferred from the impurity temperature provided by the CXS measurements [10,18]. The impurity temperatures are expected to be somewhat higher than the deuteron temperatures when the plasma is collisionally heated, however there are differences between the JETPEAK calculations for the deuteron temperatures and the ones performed in TRANSP [19], detailed in the appendix. These are insignificant for the majority of samples for which the impurity temperatures exceed deuteron temperatures by only a few percent, as is the case in baseline plasmas. For high plasmas with a high power to density ratio, such as hybrid scenario plasmas, TRANSP predicts carbon to deuterium temperature ratios up to 1.13 in the plasma core (at a normalised radius ρ=0.2), as compared to 1.065 for JETPEAK [19].

3. Comparison of results

Figures 1 and 2 show the measured total neutron rates versus the predictions from TRANSP and ASCOT respectively. The neutron rates were measured using the JET neutron monitors, which have been retrospectively recalibrated [20]. For both sets of results the dispersion of the ratio of the predicted over the measured neutron rates spans a factor 2. For the TRANSP runs the neutron rates are systematically over-predicted, with an average over-prediction of 31%. In the ASCOT case the neutron rates are on average over-predicted by 8%. On average, the TRANSP predictions for the total neutron rate are ~20% above those by ASCOT. This difference is due dominantly to the beam-thermal component, which is on average 27% higher for TRANSP. The beam-beam neutron rates are in fair agreement, TRANSP calculations being on average some 11% higher than ASCOT. The thermal neutron rates from TRANSP are on average 20% higher than the one calculated by ASCOT. Since the local thermal DD neutron rate is $r_{nDDth}=0.5n_D^2<\sigma_{DD}v>$, where n_D is the deuteron density, σ_{DD} the cross section for the $D+D\rightarrow{}^3He+n$ reaction [15] and the velocity average is taken over a Maxwellian distribution characterised by a temperature equal to T_D, it becomes clear that significant differences exist between the deuteron density and/or temperature profiles used in the two codes. The effects of any differences in T_D are exacerbated by the strong dependence of $<\sigma_{DD}v>$ on T_D, especially at low T_D. Differences are also seen in the total deposited power and in the different components of neutron production.

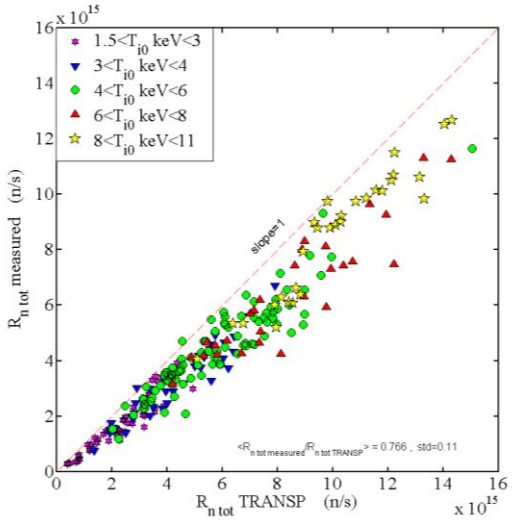

Fig.1. Measured total neutron rate versus TRANSP calculations, as in ref.[1]. The average ratio of measured to calculated neutron rates is 0.766 with a standard deviation of 0.11. The symbols refer to classes of central carbon impurity temperature

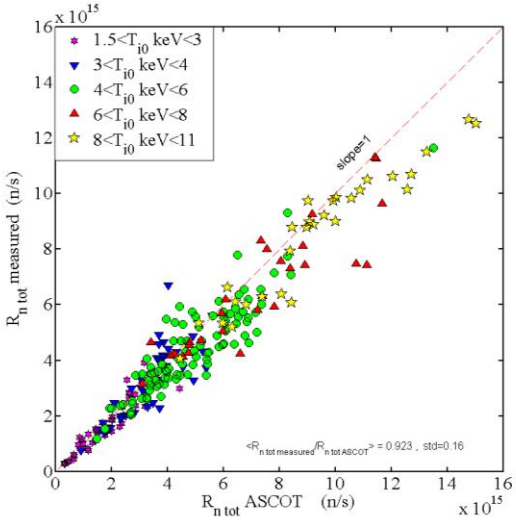

Fig. 2. Measured total neutron rate versus ASCOT calculations. The average ratio of measured to calculated neutron rates is 0.923 with a standard deviation of 0.16. The symbols refer to classes of central carbon impurity temperature

In figure 3, the deposited powers Q_{es} to the electrons (blue) and Q_{is} to the ions (red) inside of the radial locations ρ_ψ=0.3, 0.6 and 1 are shown. The flux coordinate ρ_ψ used here is defined as $\rho_\psi=(\psi/\psi_{LCFS})^{1/2}$ where ψ is the poloidal flux between the magnetic axis and the flux surface under consideration and ψ_{LCFS} is the poloidal flux between the magnetic axis and the last closed flux surface (LCFS), which defines the confined plasma volume. There are clear differences in the power deposition, as for most of the samples (except for the highest power cases) the core power deposition to ions and electrons is higher for the TRANSP results than for the ASCOT results. Fig.4a shows an example of total heat deposition profiles for TRANSP (red) and ASCOT (blue). The total power deposition (ρ_ψ=1), while not identical for both sets of code calculations, is fairly similar, with no systematic differences at low to medium power (up to ~5MW). This observation indicates a broader power deposition for ASCOT than for TRANSP. As already noted, these differences are not due to any differences between the atomic physics models used and hence must result from differences in the profiles and/or equilibria. A higher power fraction deposited in the hot core, as generally the case with the TRANSP simulations, will result in higher fast ion densities and hence higher beam-plasma neutron rates. We note that at high power and high total neutron rates ($R_{ntot}>10^{16}$n/s), which correspond to hybrid scenario plasmas, the power depositions of the two codes are in fair agreement, as are the predicted neutron rates.

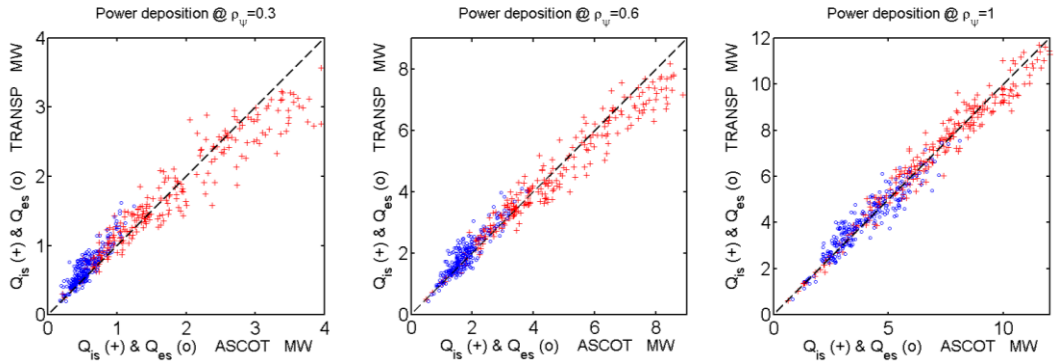

Fig. 3: Comparison of total power deposition for electrons (blue o) and ions (red +) for the ASCOT and TRANSP calculations at three radial positions, ρ_ψ =0.3,0.6 & 1.

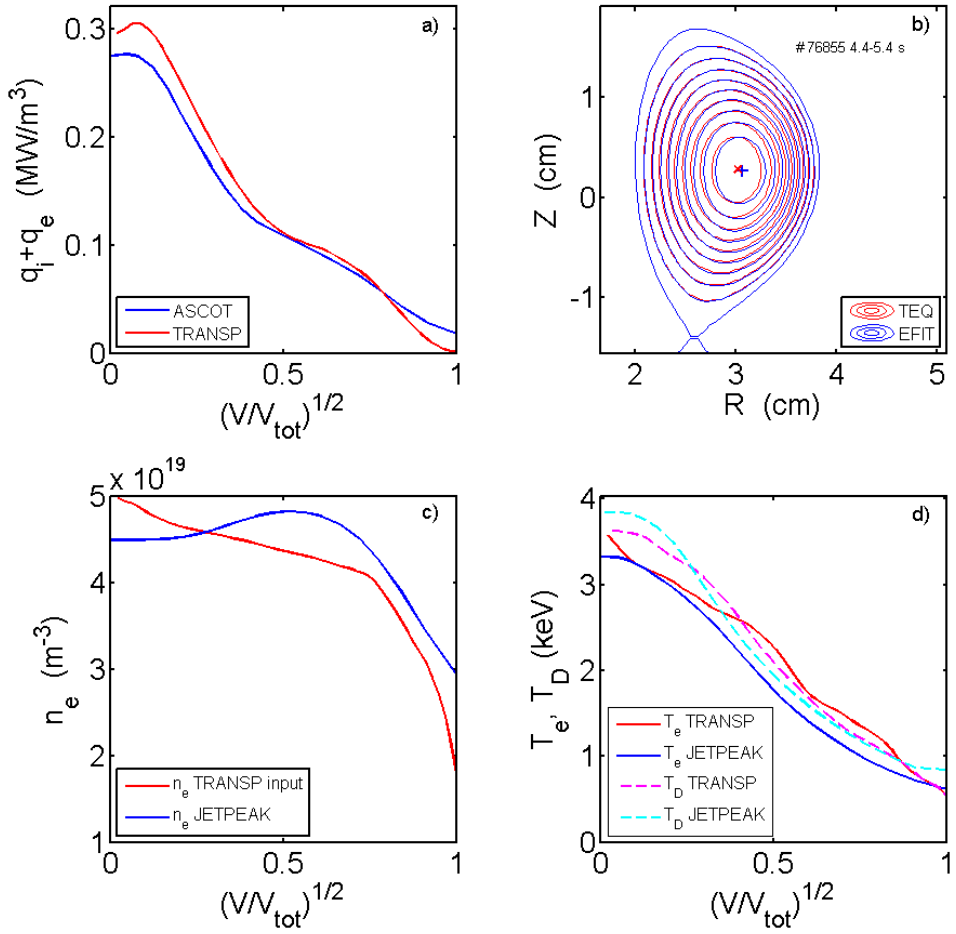

Fig.4. Example of a) total heat deposition profiles, b) TEQ (red) and EFIT (blue) equilibria, c) electron density profiles used in TRANSP (red) and ASCOT (blue), d) electron and ion temperature profiles for JET pulse 76855, sampling time interval 4.4-5.4 seconds.

Fig.4b shows that there are differences between the equilibria used by the two heating codes. The differences between the major radii can be as large as 6 cm, i.e. 5% of the major radius (fig.5a). More striking are large systematic differences in the elongation of the core flux surfaces (fig. 5b). The volumes within ρ_ψ=0.3 are systematically larger by ~0.5m^3 in TRANSP, representing a significant 10% in the core part of the plasma that produces the majority of neutrons (fig.5c). The case shown in fig.4 is marked with red circles in fig.5. While the elongations at the magnetic axis differ, the differences rapidly wane away with distance from the magnetic axis, vanishing at the last closed flux surface (LCFS). This is due to TEQ being a fixed boundary equilibrium code using the LCFS determined by EFIT as the plasma boundary.

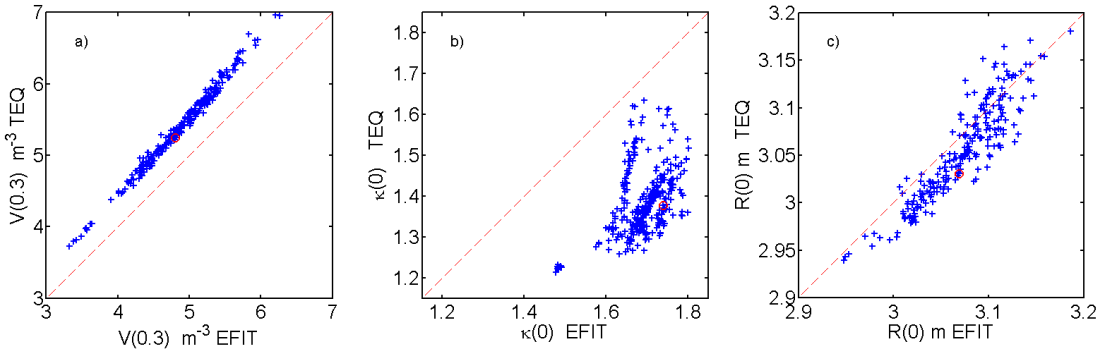

Fig.5 Comparison of equilibrium quantities between TEQ and EFIT. a) volume of plasma inside at ρ_ψ=0.3, b) elongation of flux surfaces in the centre of plasma, c) radial position of magnetic axis. The red circles correspond to the example in fig.4.

Fig.4c and 4d show examples of density and temperature profiles used as TRANSP and ASCOT inputs for the same pulse. The density profiles used for ASCOT, plotted as a function of the square root of local plasma volume normalised to the total volume (in order to give a sense of the volumes affected by the differences), are significantly above those used in the TRANSP calculations and are also less peaked. This is the case for the majority of samples and appears to be a feature of the way the profiles for the TRANSP calculations were mapped. The temperature profiles can also differ locally in magnitude by ±10% and sometimes more.

The density profiles used in TRANSP have, as shown in fig.6, typically a lower volume average density, on average by 6%, than those in JETPEAK, while having a higher core density, on average by 4%, leading to density peaking factor $n_e(0)/\langle n_e \rangle$ exceeding that in JETPEAK by 11% on average. Similar, albeit smaller differences exist for the electron temperatures. The volume average electron temperatures used by TRANSP tend to be higher than those used in ASCOT by some 3% and the core temperature by some 2%, contributing to lengthened slowing down times and higher beam-thermal neutron rates. There are no major systematic differences between deuterium ion temperatures, except at the highest temperatures ($T_i(0)$>6 keV), which also correspond to the highest powers and neutron rates, as shown in fig.7. For these cases TRANSP ion temperatures are between 0 and 10% lower than those in JETPEAK. The differences in the calculation of the underlying deuteron temperature from the measured carbon ion

temperature, presented in the appendix, have contributed up to ~6.5% to the TRANSP/ASCOT ratios of core deuteron temperatures [19]. If the main ion temperature was calculated in TRANSP as it is in ref [10], the resulting total neutron rates would be at most ~2% higher, i.e. the change would at best be marginal. The effect on the thermal neutron rate in plasma with T_D>5keV is easy to calculate and generally below 10%, representing less than 1% of the total neutron rate. The effect on the beam-plasma neutron rates, which depend on both the ion energies and the background plasma ion temperature, and can be estimated using a simple slowing down calculation like the one presented in ref[1], fig.4, is always below 1.5%.

The differences in equilibria and profiles lead naturally to the conjecture that they may have an important, if not dominant, effect on the calculations of the deposition profiles and the neutron rates. In table 1 we show how the ratios of the predicted neutron rates (TRANSP prediction / ASCOT prediction, denoted T/A) for the neutron rates and the ratios of the deposited power depositions at ρ_ψ=0.3 and ρ_ψ=1 (total deposited power) correlate with the ratios of equilibrium and profile parameters presented above.

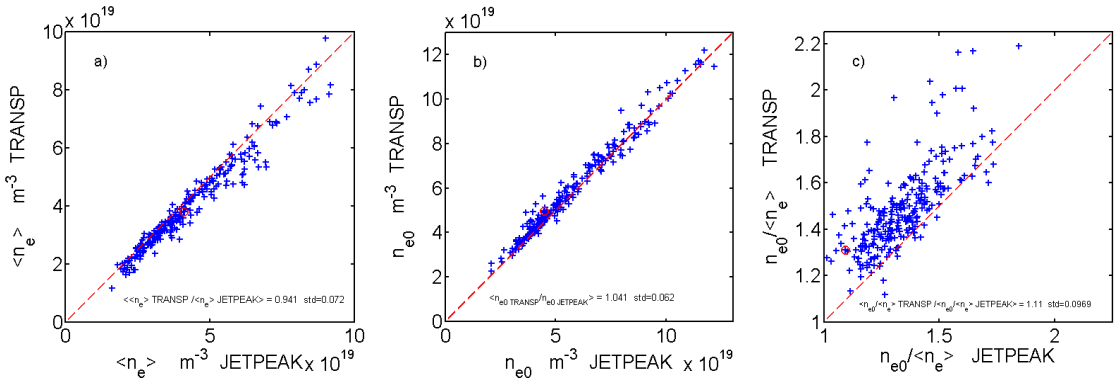

Fig.6. a) Volume average electron density $<n_e>$ used in TRANSP vs that used in the ASCOT calculations. $<n_e>_{TRANSP}/<n_e>_{ASCOT}$=0.94, standard deviation std=0.072
b) Core electron density used in TRANSP vs that used in ASCOT.
$<n_{e0}>_{TRANSP}/<n_{e0}>_{ASCOT}$=1.042, std=0.062
c) Density peaking factor of TRANSP density profiles vs that in ASCOT.
$<n_{e0}/<n_e>>_{TRANSP}/<n_{e0}/<n_e>>_{ASCOT}$=1.11, std=0.097
The red circles correspond to the example in fig.4.

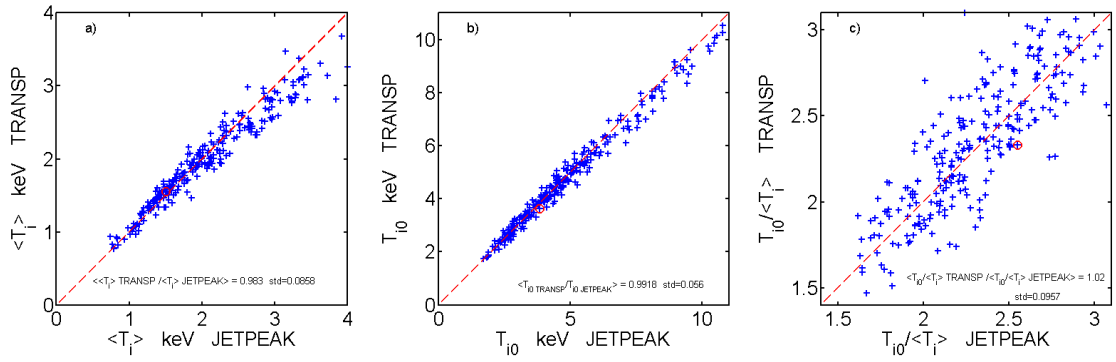

Fig.7. a) Volume average deuterium temperature used in TRANSP vs that used for the ASCOT calculations, $<T_D>_{TRANSP}/<T_D>_{ASCOT}=0.98$, standard deviation std=0.085
b) Core deuterium temperature used in TRANSP vs that used in ASCOT.
$<T_{D0}>_{TRANSP}/<T_{D0}>_{ASCOT}=0.99$, std=0.056
c) Deuterium temperature peaking factor of TRANSP density profiles vs that in ASCOT. $<T_{D0}/<T_D>>_{TRANSP}/<T_{D0}/<T_D>>_{ASCOT}=1.02$, std=0.096
The red circles correspond to the example in fig.4.

Table 1: Correlation coefficients (%), from the top line to the bottom line, between the TRANSP and ASCOT calculated ratios of the total , beam-thermal, thermal, beam-beam neutron rates, core and total heat deposition (Q_{dep}) with a selection of parameters. Quantities between brackets represent volume averages, quantities subscripted 0 refer to values at the magnetic axis, quantities annotated with (T/A) are TRANSP/ASCOT ratios. $\omega_{\varphi 0}$ is the core toroidal rotation frequency and n_D refers to the deuteron density. Darker tones correspond to stronger correlations. Correlation coefficients below 0.1 are insignificant and are blanked out.

	R_{ntot} (T/A)	R_{nbt} (T/A)	R_{nth} (T/A)	R_{nbb} (T/A)	Q_{dep}(0.3) (T/A)	Q_{dep}(1) (T/A)	$<n_e>$ (T/A)	n_{e0} (T/A)	$<n_D>$ (T/A)	n_{D0} (T/A)	n_{D0}/n_{e0} (T/A)	$<n_D>/<n_e>$ (T/A	$<T_D>$ (T/A)	T_{D0} (T/A)	$n_{e0}/<n_e>$ (T/A)	R_0 (T/A)	κ_0 (T/A)	V(0.3) (T/A)	n_{e0}	T_{e0}	T_{D0}	$\omega_{\varphi 0}$
R_{ntot} (T/A)		95	69	43	37	13	−27		15	32	−13	21	15	13	23		−12	16		−21	−33	−33
R_{nbt} (T/A)	95		53	50	31	11	−32			28	−22				26	17		27			−16	−23
R_{nth} (T/A)	69	53		−13	22			12	41	13	22	38	43	25		−23	−33		13	−29	−41	−32
R_{nbb} (T/A)	43	50	−13		56	22	−50	−24		55	−41	17			30				33		−16	−14
Q_{dep}(0.3) (T/A)	37	31	22	56		30	−30		40	76	−18	45	23		29	−34	−54		44	−36	−48	−24
Q_{dep}(1) (T/A)	13	11		22	30		14		17	18		18			−11	−19		−20	14	13		

The ratio of the total core power depositions $Q_{dep}(0.3)$ is clearly strongly correlated with the ratios the equilibria variables used as seen with its correlations with κ_0 and R_0, as well as the differences with the ratios of volume average deuteron densities, density peaking factors and the purity n_{D0}/n_{e0}. The ratio of $Q_{dep}(0.3)$ also correlates with core densities and core temperatures (taken from JETPEAK), indicating that the influence of differences between parameters depends on plasma conditions. This can be understood from the fact that e.g. neutral beam penetration to the core decreases with density

roughly as exp(-η<n_e> a), where the beam stopping coefficient η mainly depends of the injection energy and a is the minor radius, causing high density plasmas to be more strongly affected than low density plasmas.

The ratio of the power deposition at ρ_ψ=0.3 can be regressed with just those two parameters, the ratios of central deuteron densities n_{D0} and flux surface elongation κ_0, as seen in fig.8. We use an automatic regression routine that uses all possible combinations of regression variables out of a set of more than 20, including those shown in table 1 and ranks them by the quality of fit given as the standard deviation of the difference between the input for the response variable (or dependent variable), here $\log(Q_{dep}(0.3)_{TRANSP}/Q_{dep}(0.3)_{ASCOT})$ and the value provided by the regressions. The usage of further parameters from table 1 for the multivariate regression seen in fig.8 only marginally improves the regression. It corresponds to

$$Q_{dep}(0.3)_{TRANSP}/\ Q_{dep}(0.3)_{ASCOT} \propto (n_{D0\ TRANSP}/n_{D0\ ASCOT})^{0.48}\ (\kappa_{0\ TEQ}/\kappa_{0\ EFIT})^{-0.97} \qquad \text{eq.1}$$

The exponents of this power law regression show how sensitively the response variable depends on the regression variables. As important as the exponents are the contributions of variations in the regression variables to the variations of the response variable, i.e. their relevance, as well as their significance, defined below.

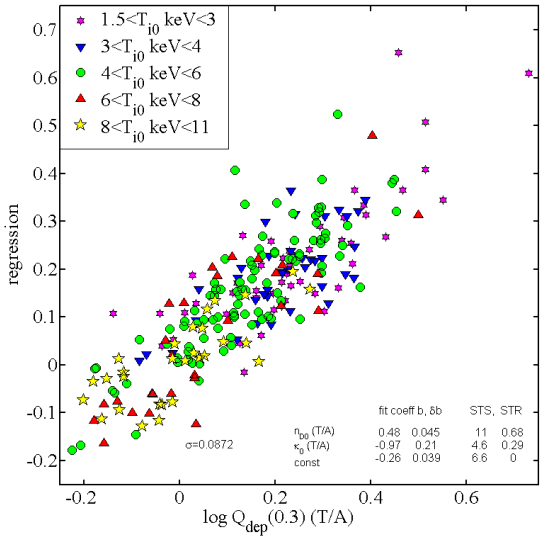

Fig.8 Power law regression of the ratios of $Q_{dep}(0.3)(T/A)=Q_{dep}(0.3)_{TRANSP}/Q_{dep}(0.3)_{ASCOT}$ using the ratios noted $n_{D0}(T/A)=n_{D0\ TRANSP}/n_{D0\ ASCOT}$ and $\kappa_0(T/A)=\kappa_{0\ TEQ}/\kappa_{0\ EFIT}$. The columns refer from left to right to the fit coefficients (b), which are the exponents of the power law regression, their uncertainties (δb), the statistical significance STS and the statistical relevance STR defined in the main text. The label σ=0.0872 is the standard deviation of the regression.

The legend at the bottom of fig.8 (and beyond) includes the linear regression coefficients b_i, their errors δb_i for each regression variable v_i (here $v_1 = \log(n_{D0\ TRANSP}/n_{D0\ ASCOT})$ and $v_2 = \log(\kappa_{0\ TEQ}/\kappa_{0\ EFIT})$), as well as the statistical significance $b_i/\delta b_i$, labelled STS, and the statistical relevance labeled STR. The STR of variable v_i is defined as $b_i\sigma_i/\sigma_{resp}$, where σ_i is the standard deviation of regression variable v_i and σ_{resp} is the standard deviation of the response variable. (The quantities b_i, δb_i, σ_i, σ_{resp} are returned by the multivariate regression routine used). The STR indicates what fraction of the variations of the response variable can be attributed to the variations of the regression variable v_i.

The STR's for the two regression variables are 0.68 and 0.29 respectively, showing that the variations of the differences in density profiles are the most important factor for explaining the variations of differences in core heat deposition. We should of course not assume that the core density and elongation differences, as such, are the 'causes' of the deposition profile differences. The ratios of core elongations should be seen as proxies for the differences in the equilibria overall.

The power law regressions in figs. 9-12 confirm that the TRANSP/ASCOT ratio of the beam-thermal, thermal-thermal, beam-beam and total neutron rates have, as expected, dependencies on the ratios of core power depositions, densities and equilibrium quantities, showing that the systematic differences in the neutron rates, too, can be largely accounted for by differences in the equilibria and profiles. In particular, the beam-thermal neutron rates (fig.9) can be regressed with just two parameters:

$$R_{nbtRANSP}/ R_{nbtASCOT} \propto (Q_{dep,TRANSP}(0.3)/Q_{dep,ASCOT}(0.3))^{0.44} (\kappa_{0\ TEQ}/\kappa_{0\ EFIT}) \qquad \text{eq.2}$$

$Q_{dep,TRANSP}(0.3)/Q_{dep,ASCOT}(0.3)$ and $\kappa_{0TEQ}/\kappa_{0EFIT}$, have STR's of 0.68 and 0.45 respectively. $Q_{dep,TRANSP}(0.3)/Q_{dep,ASCOT}(0.3)$ is the single most important variable for determining $R_{nbtRANSP}/R_{nbtASCOT}$. A marginally better regression (σ=0.095 instead of 0.096) than expressed in eq.2 without this variable requires 5 variables: the TRANSP/ASCOT ratios of $<n_e>$, $<T_e>$, $Q_{dep}(1)$, V(0.3) with STRs equal to 0.42, 0.18, 0.35 and 0.25 respectively, as well the core plasma rotation frequency $\omega_{\varphi 0}$ with an STR of 0.23. Clearly, both differences in the profiles, especially the density profiles, are important, as well as differences in the equilibria and the total deposited power. The question as to which is most important cannot be unambiguously answered, as the mapping and fitting of the experimental profiles cannot be thought of as being independent of the equilibria to which they are being mapped and fitted.

The TRANSP/ASCOT ratios of the thermal neutron rates are seen in fig.10 to depend on a combination of plasma purity ratios $<n_D>/<n_e>$ (T/A) and as expected on the ratios of deuteron temperatures $<T_D>$ (T/A) and to a lesser extent on ratios of core elongation and core volumes, V(0.3), as seen from the STR's in the figure legend. The ratios of beam-beam neutron rates in fig.11 are well regressed by combinations of ratios of electron and deuteron densities, as well as by the core density itself. Finally, fig.12 shows a 5-parameter regression for the ratios of the total neutron rates where the ratios of $<T_D>$ and V(0.3) have the highest statistical relevance, as seen in the legend.

Of course, intrinsic differences between the two codes do exist, however the differences known so far have a smaller influence on the neutron rates, as suggested by ref.13 and the comparison of the underlying deuterium temperatures from the measured impurity temperatures, presented in appendix 1. The slightly lower deuteron temperatures inferred by TRANSP on the basis of the carbon temperatures have the effect of compensating to a small extent (<2%) the over-prediction of the total neutron rates, in particular the thermal neutron rates, as can be seen from the exponent, equal to 2, for $<T_D>$ in fig.10.

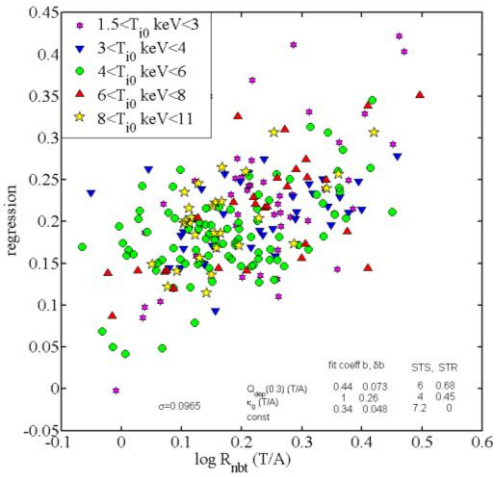

Fig.9 Power law regression for the TRANSP/ASCOT ratios of the beam-thermal neutron rates (legend explained in fig.7). The symbols represent classes of central carbon impurity temperature.

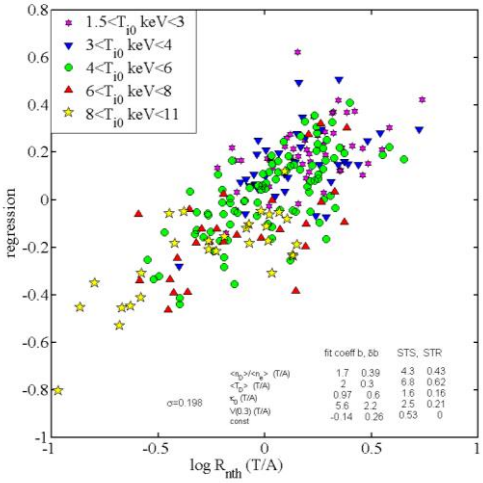

Fig.10 Power law regression for the TRANSP/ASCOT ratios of the thermal-thermal neutron rates.

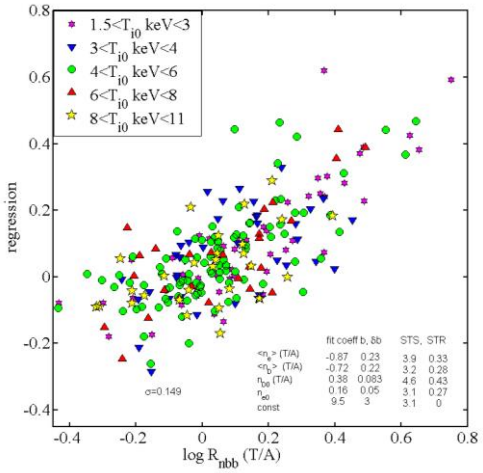

Fig.11 Power law regression for the TRANSP/ASCOT ratios of the beam-beam neutron rates

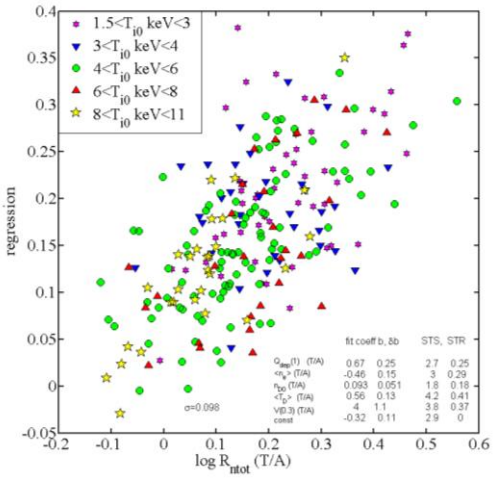

Fig.12 Power law regression for the TRANSP/ASCOT ratios of the total neutron rates

6. Discussion and conclusions

Large differences between the two simulations using the two codes are obtained between the two codes using different equilibria and most importantly, different ways of mapping the raw profiles. The differences between the EFIT and the TEQ equilibria and the differences between profiles used in TRANSP and those in JETPEAK were under-appreciated and under-investigated at the time the study reported in ref. [1] was performed. The possibility and motivation for the study presented here only arose after the software for automatic ASCOT calculations was implemented. The TRANSP-calculated dataset showed a systematic over-prediction, by an average 31%, of the measured neutron rates. The ASCOT calculations, based on profiles in the JETPEAK database feature an average over-prediction of approximately 8%. Significant differences in the heat deposition profiles are observed. In the TRANSP simulations core heat deposition was significantly higher than in the ASCOT calculations and directly traceable to the differences in equilibria and profiles, especially the core electron and/or deuteron densities. In the light of the ASCOT calculations, the systematic shortfall in neutron rates reported in ref. [1] as compared to the TRANSP calculations, may have been undeservedly called a 'neutron deficit', thereby suggesting the existence of significant and ununderstood fast ion loss processes in the plasma. The 8% average shortfall obtained with ASCOT using JETPEAK profiles may be explained by the many possible mechanisms reviewed in ref. [1], as well as by measurement, calibration, equilibrium and mapping errors and is not large enough to be suggestive of a systematic 'neutron deficit'. It also shows, together with recent successful TRANSP simulations of JET-ILW baseline and hybrid scenario plasmas [21], that we can be confident in the predictive and interpretive usage of the two codes for the JET DTE2 campaign. This experience shows that meticulous preparation, mapping and the choice of the plasma equilibrium are more important than the intrinsic differences between ASCOT and TRANSP. We understand that the options used for mapping and fitting the profiles for ref. [1] are now disused and replaced by the rigorous OMFIT procedure [22]. Finally, the method used here can also be applied to bring to light intrinsic differences between the codes, if the TEQ equilibria and the profiles used for the TRANSP calculations are used as inputs for ASCOT.

Acknowledgments

This work has been carried out within the framework of the EUROfusion Consortium and has received funding from the Euratom research and training programme 2014-2018 and 2019-2020 under grant agreement No 633053. The views and opinions expressed herein do not necessarily reflect those of the European Commission.

References

[1] H. Weisen et al. 2017 Nuclear Fusion 57 076029
[2] A. Pankin et al. 2004 Comput. Phys. Commun. 159 157-184
[3] Breslau, J., Gorelenkova, M., Poli, F., Sachdev, J., Yuan, X. & USDOE Office of Science. TRANSP. Computer software. USDOE Office of Science (SC), Fusion Energy Sciences (FES) (SC-24). 27 June 2018. Web. doi:10.11578/dc.20180627.4.
[4] R. Andre et al. 2006 New MHD Equilibrium Solver Options in TRANSP, American Physical Society 48th Annual Meeting of the Division of Plasma Physics, Philadelphia, PA, October 30 – November 3 2006, JP1.129
Also: ttps://w3.pppl.gov/~pshare/help/body_transp_hlp.html#outfile88.html
[5] J. Mailloux et al. "Overview of JET results for optimising ITER operation", to be published in Nuclear Fusion Special issue: Overview and Summary Papers from the 28th Fusion Energy Conference (Nice, France, 10-15 May 2021)
[6] M.N.A. Beurskens et al 2013 Nucl. Fusion 53 013001
[7] C. Giroud et al, Rev. Sci. Instrum. 79 (2008) 525
[8] ITER Physics Expert Group on Confinement and Transport, ITER Physics Basis, Chapter 2, Nuclear Fusion, 39 (1999) 2175
[9] P. Sirén et al 2019 JINST 14 C11013
[10] H. Weisen et al. 2020 Nucl. Fusion 60 036004
[11] E. Hirvijoki et al. 2014 Comput. Phys. Commun. 185 1310-1321
[12] O. Asunta et al. 2015 Comput. Phys. Commun. 188 33-46
[13] P. Sirén et al, "Comprehensive benchmark studies of ASCOT and TRANSP-NUBEAM fast particle simulations" paper P4.1026, 46th European Physical Society Conference on Plasma Physics (EPS 2019), Milan, Italy, July 8-12, 2019, http://ocs.ciemat.es/EPS2019PAP/pdf/P4.1026.pdf
[14] General Atomics EFIT equilibrium and reconstruction fitting code https://fusion.gat.com/theory/Efit
[15] H.-S. Bosch, G. M. Hale 1992 Nucl. Fusion 32 611
[16] R. K. Janev 1989 Nucl. Fusion 29 2125
[17] H. P. Summers 2004 The ADAS User Manual, version 2.6 http://www.adas.ac.uk
[18] R. Budny et. al. 1992. Nucl. Fusion 32 3 pp.429-447
[19] H.Weisen, 28th IAEA Fusion Energy Conference, Nice, France, 10-15 May 2021, "Analysis of the inter-species power balance in JET plasmas"
https://conferences.iaea.org/event/214/contributions/17320/
provisional link for 8-page paper until publication of the proceedings by IAEA:
https://docs.google.com/document/d/1Zo1zMnPqUaFLYRyMz1Joc2Qh1pcraRU_jxK0xXUv7AE/edit?usp=sharing
[20] D. B. Syme et al. 2014 Fusion Eng. Des. 89 2766-2775
[21] K.K. Kirov et al 2021 Nucl. Fusion 61 046017
[22] N.C.Logan et al, 2018, Fusion Science and Technology 74, 125-134
[23] S.D. Scott "Impurity Ti Model in TRANSP (SLVTX)", PPPL document, 4.2.2003

Appendix 1:
Comparison of ion-impurity temperature ratios in TRANSP and JETPEAK

We have made use of the dataset produced by the TRANSP calculations for ref. [1] to cross check the carbon-to-deuterium temperature ratios T_C/T_D calculated in TRANSP with those produced by the routines developed for JETPEAK [10]. The analytical formula is executed with the assumption $\alpha = \chi_C/\chi_D = 1$ where χ_C and χ_D are the carbon and deuterium heat diffusivities. In the absence of any other information on the transport regime it seems reasonable to assume that the minority species, here carbon, undergoes passive transport determined by the majority species, justifying this assumption. Fig.13 shows the ratios obtained from the analytical formula routinely used for JETPEAK, eq.18 in ref. [10], versus the TRANSP calculations in the plasma core at ρ=0.2. (Here $\rho=(\varphi/\varphi_{LCFS})^{1/2}$ where φ is the toroidal flux, is the toroidal flux coordinate, as used in TRANSP).

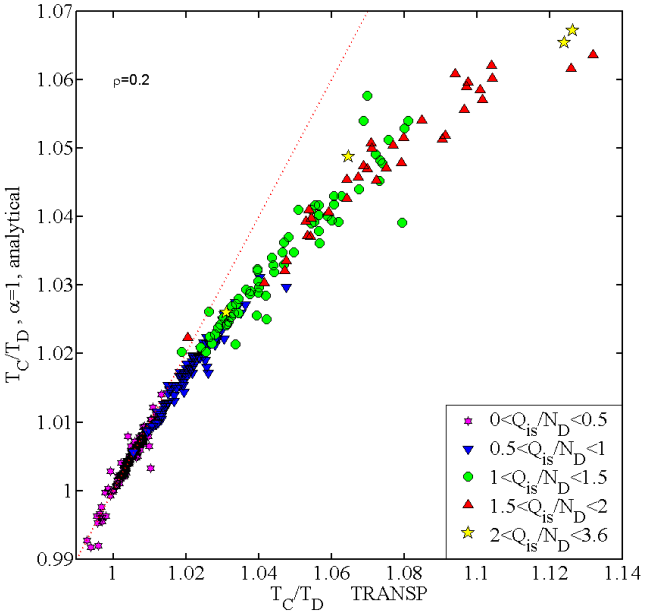

Fig.13. Ratio of the carbon-to-deuterium temperatures at ρ=0.2 using the analytical formula in ref. [10] versus the result from the TRANSP calculations for ref.[1].

The symbols refer to a measure of ion power per particle inside ρ=0.2 defined as

$$Q_{is}/N_D = 10^{-20}\frac{\int_0^{V(\rho)} q_{is}dV}{\int_0^{V(\rho)} n_D\, dV} \qquad \text{eq. A1}$$

where q_{is} is the deposited ion power density and n_D is the deuteron density showing that the ratio T_C/T_D increases with power per particle. We note that for T_C/T_D up to ~1.02 the two calculations agree well, but diverge for higher values. At the highest values of T_C/T_D the TRANSP calculations of the temperature difference T_C-T_D exceed those obtained from the analytical formula by a factor 2.

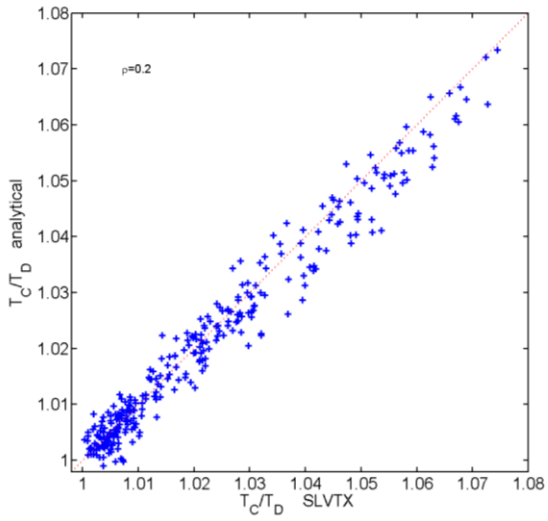

Fig 14. Comparison of T_C/T_D obtained from eq.18 in ref.[8] and the author's implementation of SLVTX.

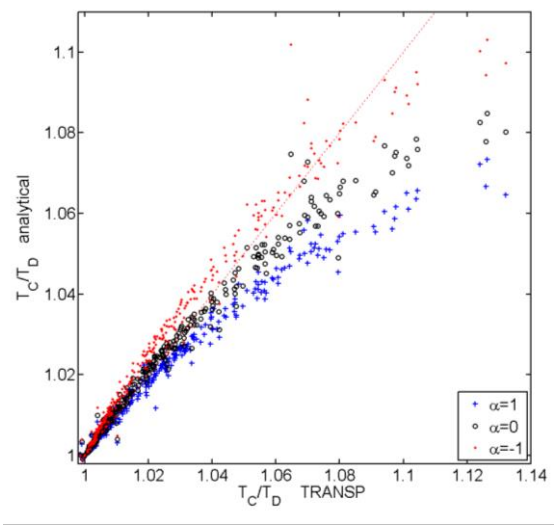

Fig. 15 Comparison of *T_C/T_D at $\rho=0.2$ using the analytical formula in ref.[8], for 3 different assumptions for* $\alpha= \chi_C/\chi_D$ *versus the result from the TRANSP calculations.*

TRANSP calculates T_C/T_D using an implementation of the SLVTX routine [24]. We have implemented a simple stationary state version ($\partial/\partial t=0$) of SLVTX and applied it to the same input data as in our own calculations based on eq.18 of ref.[10], also assuming $\alpha= \chi_C/\chi_D =1$. The two calculations provide the same results, as seen in fig.14. As a result of this we suspect an error in the TRANSP implementation of SLTVX or the implementation of a different assumption for $\alpha= \chi_C/\chi_D$. Fig.15 shows the results of the analytical formula when α=1, 0, and -1 are assumed. The choice α=-1 (red dots in fig. 15) provides good agreement, but is unphysical, suggesting that the cause of the discrepancy seen in fig.13 is an error of sign representing α or the ratio of impurity-to-main species heat fluxes in the TRANSP implementation of SLVTX.